Space Weather: The International Journal of Research and Applications

Supporting Information for

Quantifying the storm-time thermospheric neutral density variations using model and observations

E. Ceren Kalafatoglu Eyiguler[1], J. S. Shim[2], M. Kuznetsova[3], Z. Kaymaz[1], B. R. Bowman[4], M. V. Codrescu[5], S. C. Solomon[6], T. J. Fuller-Rowell[5], A. J. Ridley[7], P. M. Mehta[8] and E. K. Sutton[9]

[1] İstanbul Technical University, Faculty of Aeronautics and Astronautics, Department of Meteorology, İstanbul, TR

[2] The Catholic University of America, NASA GSFC, Greenbelt, MD, USA

[3] NASA, Goddard Space Flight Center, Greenbelt, MD, USA.

[4]Air Force Space Command Space Analysis Division, Peterson AFB, CO, USA

[5] Space Weather Prediction Center, National Oceanic and Atmospheric Administration, Boulder, CO, USA

[6] High Altitude Observatory, National Center for Atmospheric Research, Boulder, CO, USA

[7] School of Engineering, University of Michigan, Ann Arbor, MI, USA

[8] Department of Mechanical and Aerospace Engineering, West Virginia University, WV, USA.

[9]Air Force Research Laboratory, Kirtland AFB, NM, United States

Contents of this file

Introduction

This supporting information file includes:

1. Figure S1: Plot showing the orbit-averaged neutral density variations on quiet day cases, which were used for the threshold detection
2. Figures S2 to S7: For each event, the plots of i) time series of the thermospheric neutral density observations from M2017 and empirical and neutral density estimations from the physics-based models of the I-T and Kp, ii) background series for M2017 and models, iii) Shift 1 to Shift6.
3. Figure S8: MAE and RMSE from models for all events
4. Figure S9: Mean $ln(\rho_m/\ \rho_o)$, normalized standart deviation of $ln(\rho_m/\ \rho_o)$, normalized root mean square error of $ln(\rho_m/\ \rho_o)$ according to (Sutton, 2018).

5. Figure S10: Expanded form of Figure 3 of the paper with all shifts. The figure shows the ratio of average, ratio of maximum and time delays of the models after the application of baseline shifts from SH1 to SH6.
6. Figure S11: Expanded form of Figure 5 of the paper with all shifts. The figure shows the mean absolute error, normalized root mean square error and prediction efficiency of the models after the application of baseline shifts from SH1 to SH6.
7. Table S1: Runs at the CCMC Runs-on-Request system.
8. Table S2: Model inputs
9. Table S3: Quiet-time differences and ratios between the models and M2017.

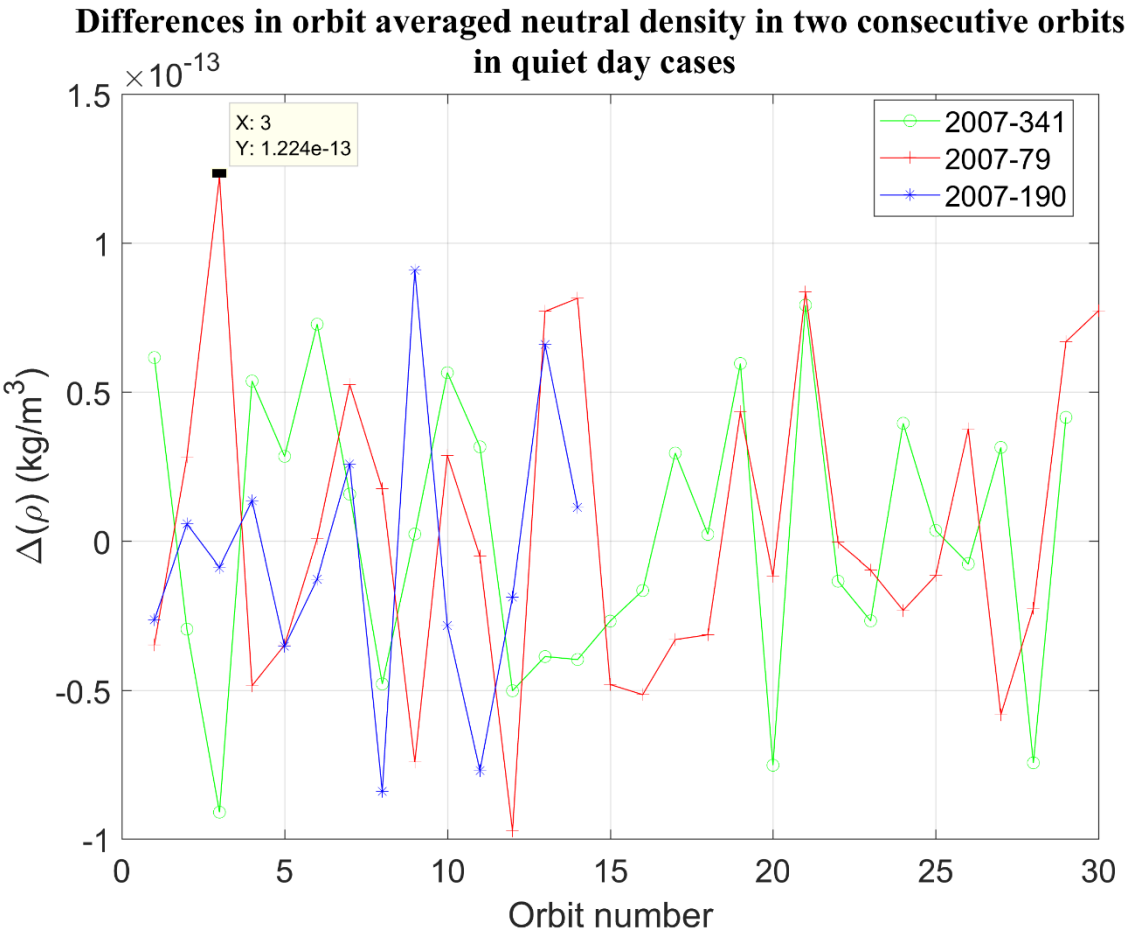

Figure S1. Differences in orbit-averaged neutral densities in two consecutive orbits on quiet day cases for the threshold detection. 2007-341: green line with circle; 2007-79 red line with plus; 2007-190, blue line with asterisk.

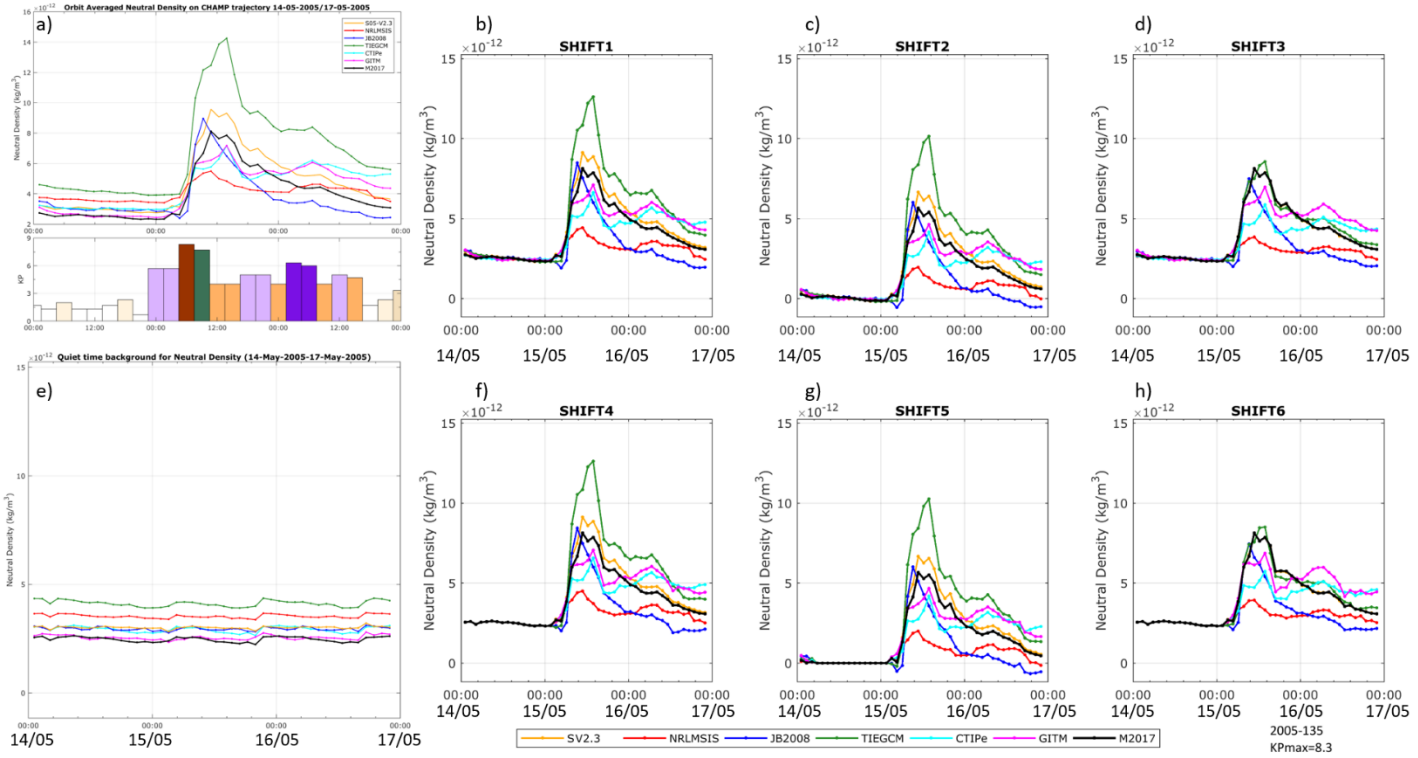

Figure S2. Event: 2005-135. First row, from left to right: a) top: Neutral density from the model and observations without shift; below: Kp index, neutral density estimations from CHAMP derived by Mehta et al. 2017 (M2017) and by Sutton (2005) (SV2.3) and the neutral density estimations from the models (NRLMSIS, JB2008, TIEGCM, CTIPe, GITM) after b) SH1, c) SH2, d) SH3. Second row, from left to right: e) Generated background series, neutral density estimations from the methods and M2017 after f) SH4, g) SH5, h) SH6. Selected quiet time: May 14, 04:30UT to May 15 02:30UT, Disturbed period: May 15, 04UT to May 16, 23:59UT.

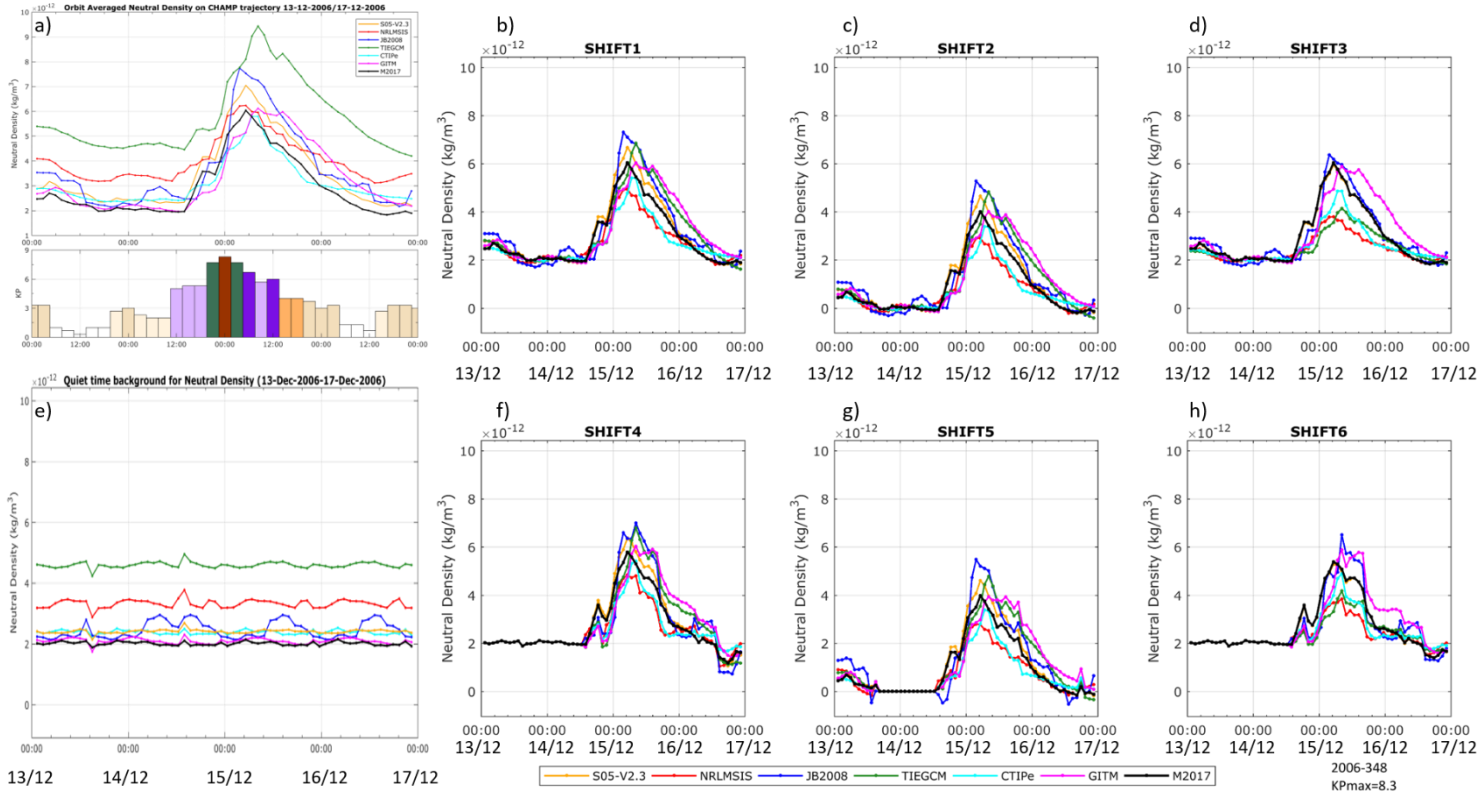

Figure S3: Event: 2006-348. Panels are the same as Figure S2. Selected quiet time: December 13, 15UT to December 14, 13:30UT, Disturbed period: December 14, 14UT to December 16, 12UT

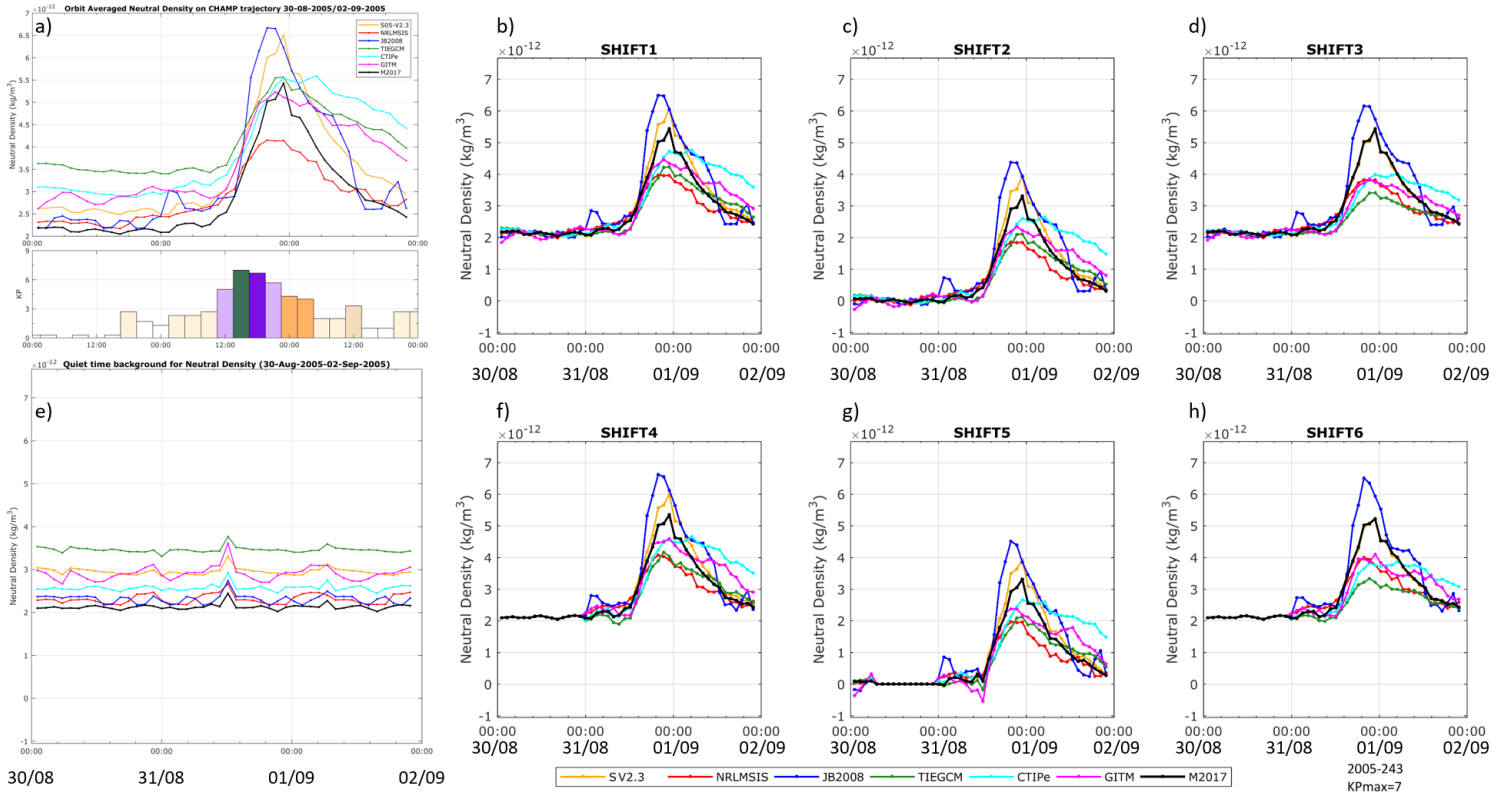

.

Figure S4. Event: 2005-243. Panels are the same as Figure S2. Selected quiet time: August 30, 06UT to August 30 23:59UT, Disturbed period: August 31, 07:30UT to September 1, 23:59UT.

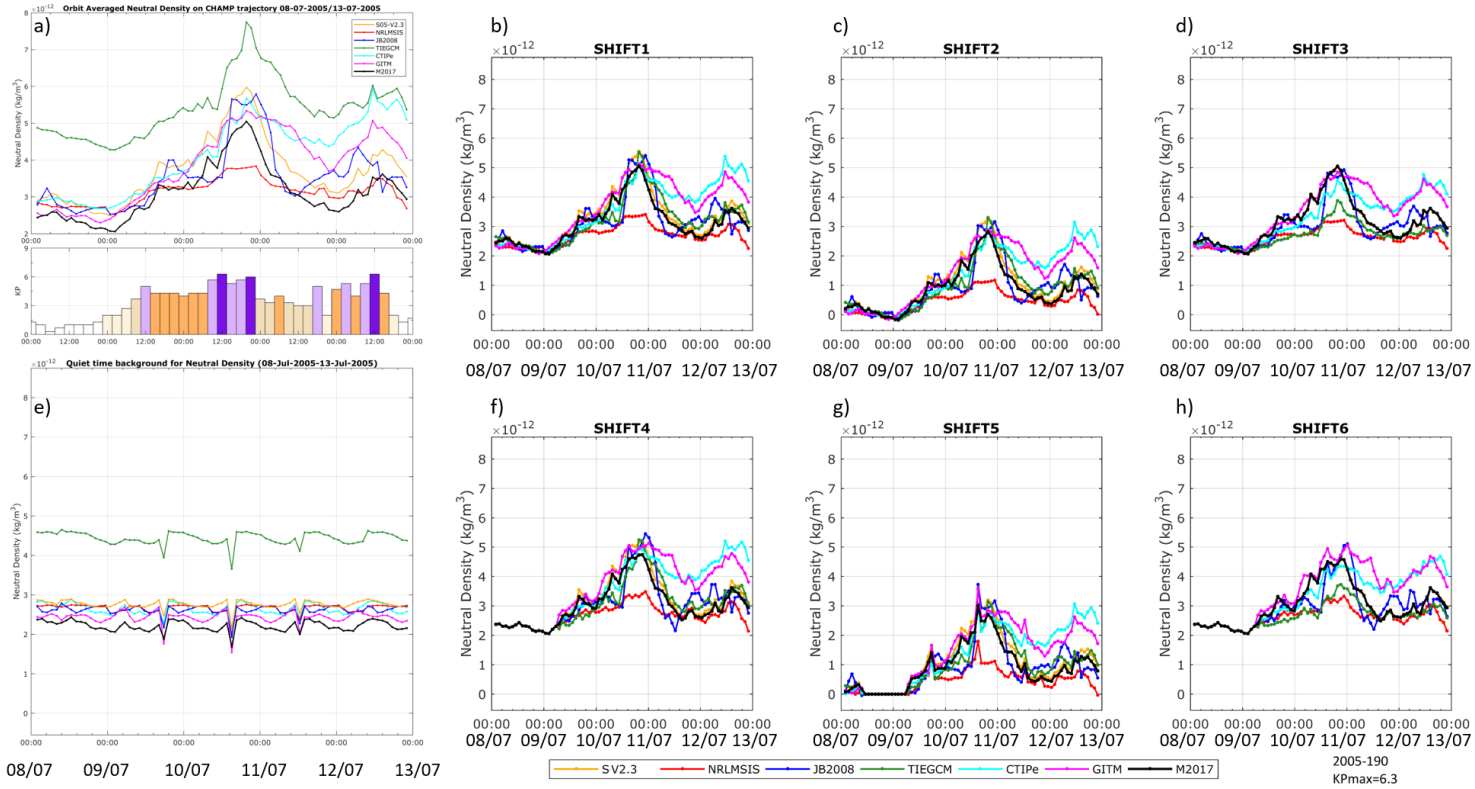

Figure S5. Event: 2005-190. Panels are the same as Figure S2. Selected quiet time: July 8, 09:30UT to July 9, 06:30UT, Disturbed period: July 9, 07UT to July 12, 00UT.

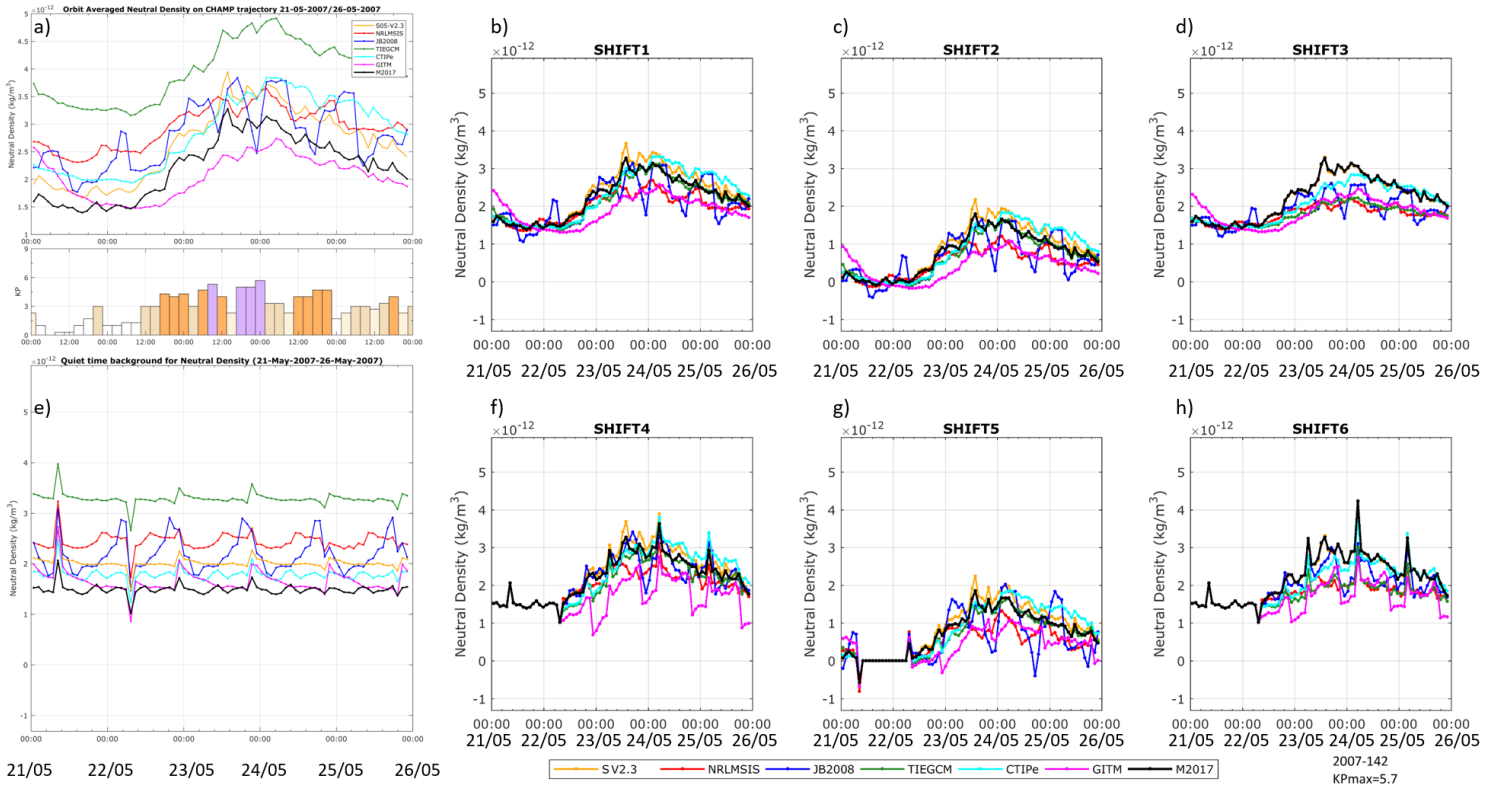

Figure S6. Event: 2007-142. Panels are the same as Figure S2. Selected quiet time: May 21, 08:20UT to May 21, 07:30UT, Disturbed period: May 22, 08:30UT to May 25, 23:59UT.

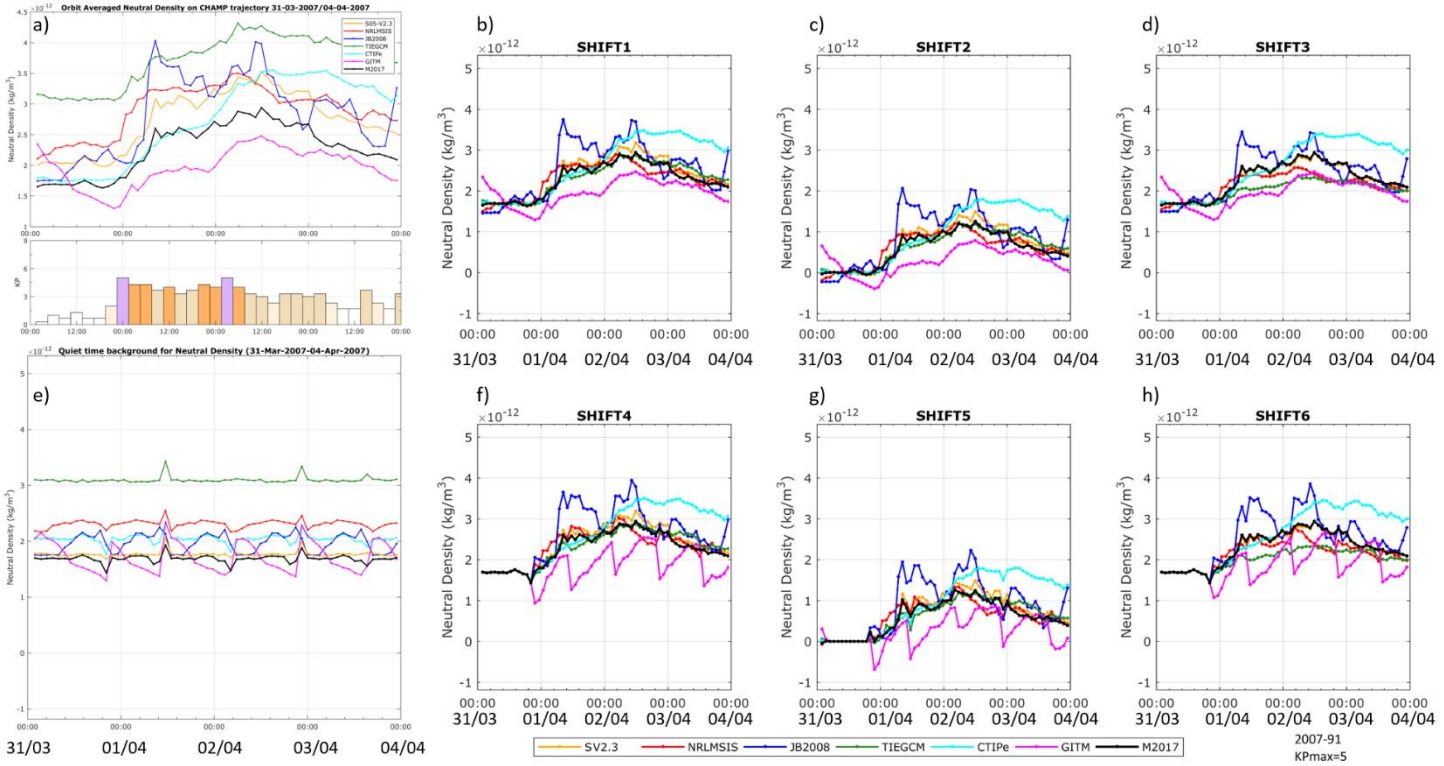

Figure S7. Event: 2007-91. Panels are the same as Figure S2. Selected quiet time: March 31, 03UT to March 31, 20:30UT, Disturbed period: March 31, 23 UT to April 3, 23:59UT.

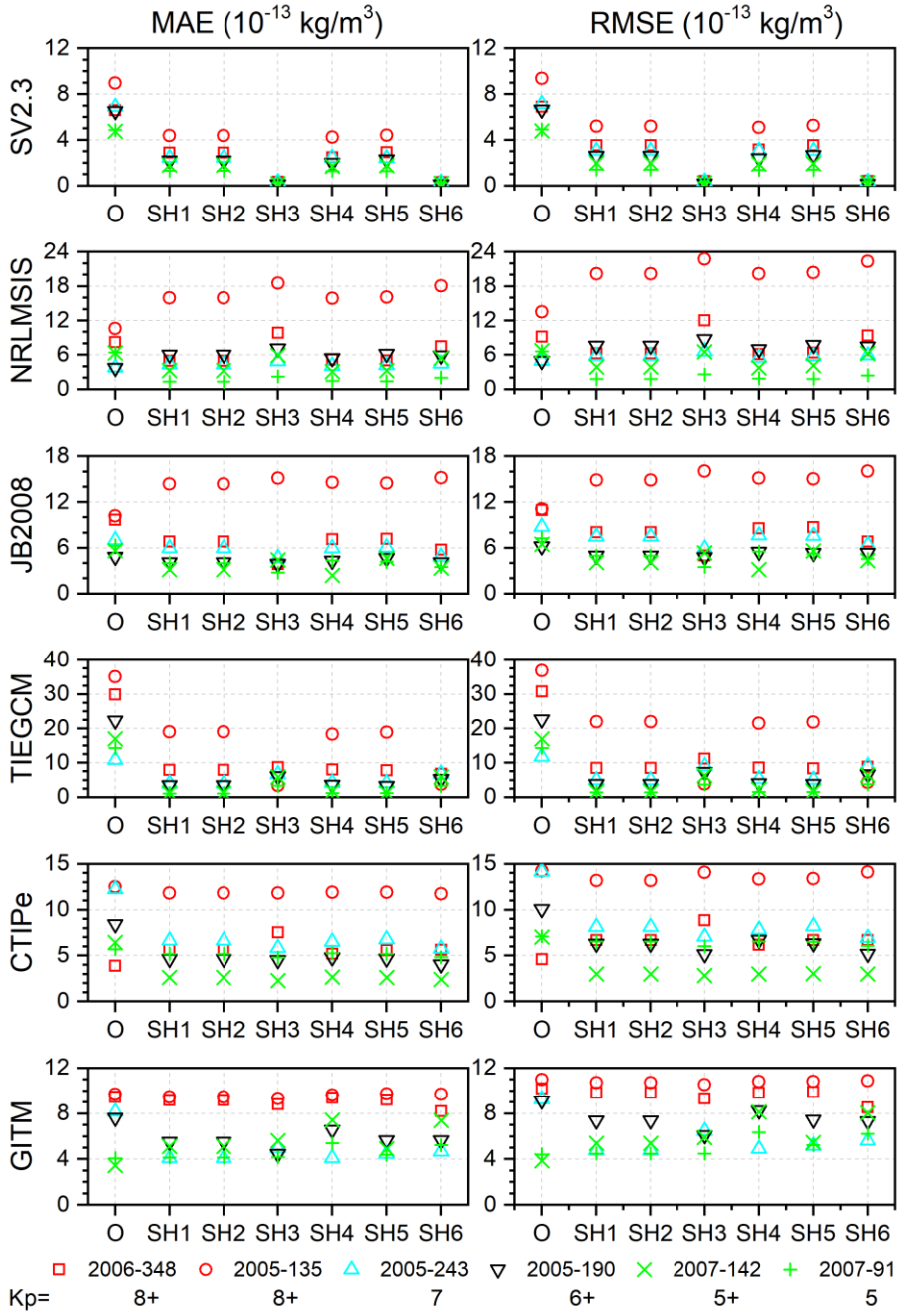

Figure S8: MAE and RMSE for all events. From top to bottom: SV2.3, MSIS, JB2008, TIEGCM, CTIPe, GITM. O denotes the results for the original, unshifted series whereas SH1 to SH6 represent the shifts from Shift1 to Shift6. Red symbols represent the severe events with high Kp; cyan denotes strong event with Kp=7; black is for 7>Kp>6; and green color is for weak events with Kp around 5. Circle represents the event 2005-135; square, 2006-348; up-triangle, 2005-243; down-triangle, 2005-190; cross, 2007-142; plus, 2007-91.

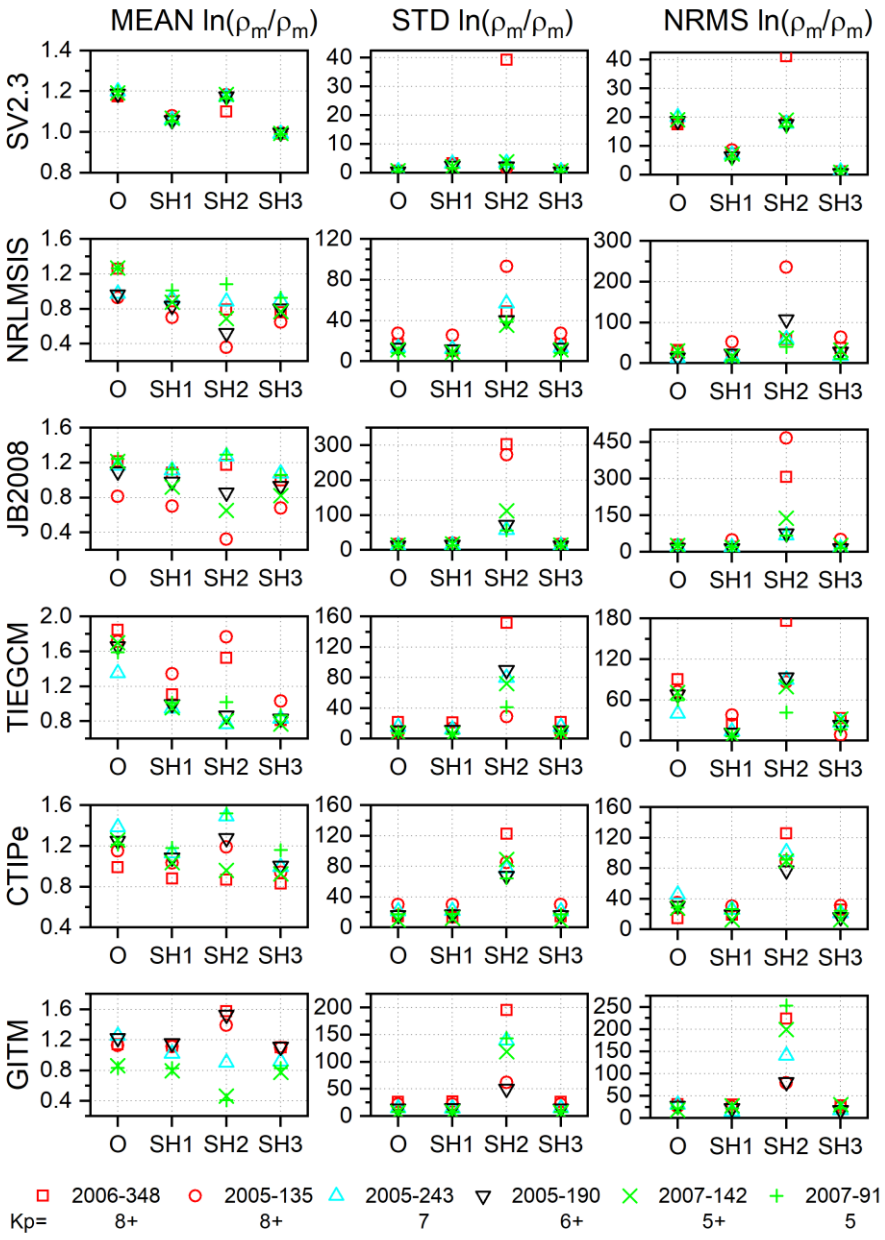

Figure S9: Mean *ln*(ρ_m/ρ_o), normalized standart deviation of *ln*(ρ_m/ρ_o) and normalized root mean square error of *ln*(ρ_m/ρ_o) according to (Sutton, 2018). The symbols and colors are the same as in Figure S8.

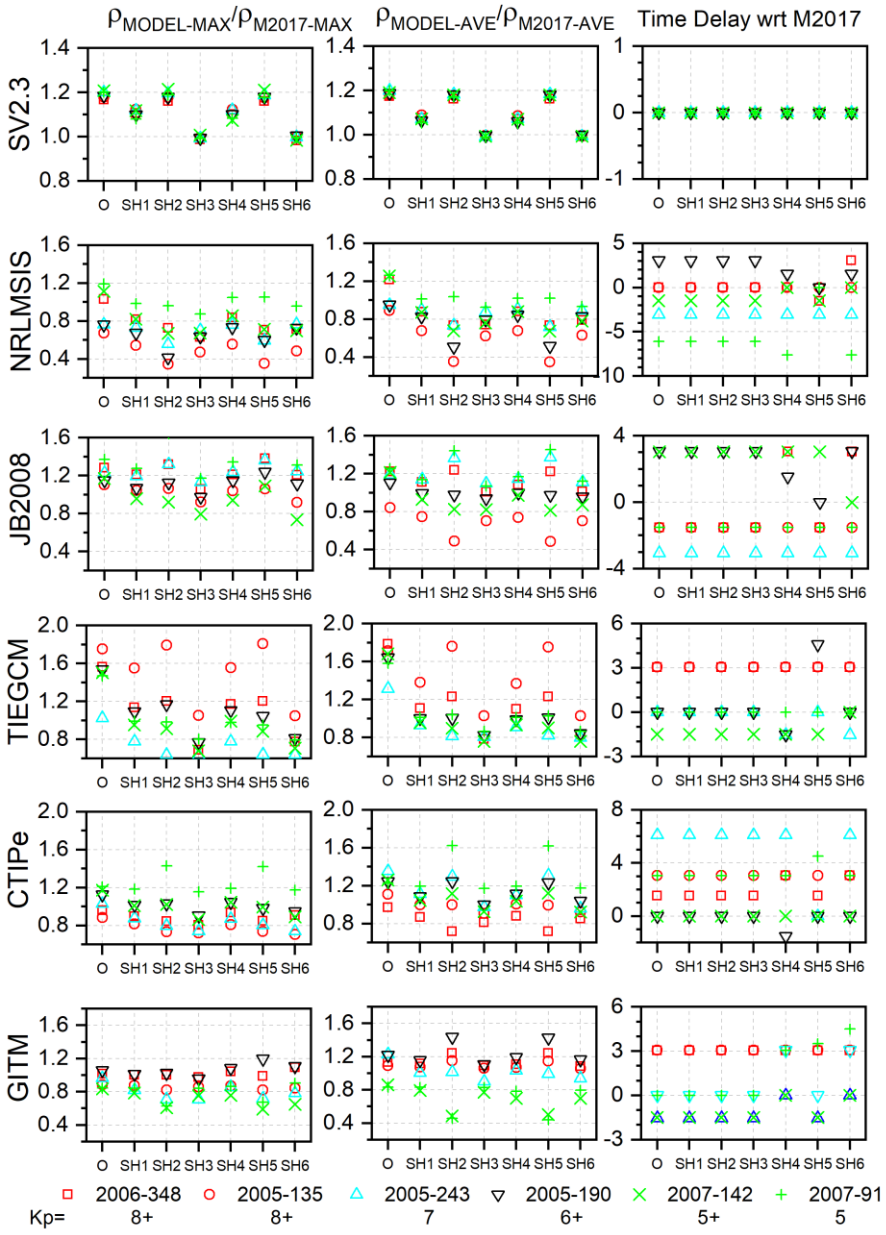

Figure S10: The expanded form of Figure3 with all shifts. O denotes the results for the original, unshifted series whereas SH1 to SH6 represent the shifts from Shift1 to Shift6. The color coding and symbols are the same as Figure S8.

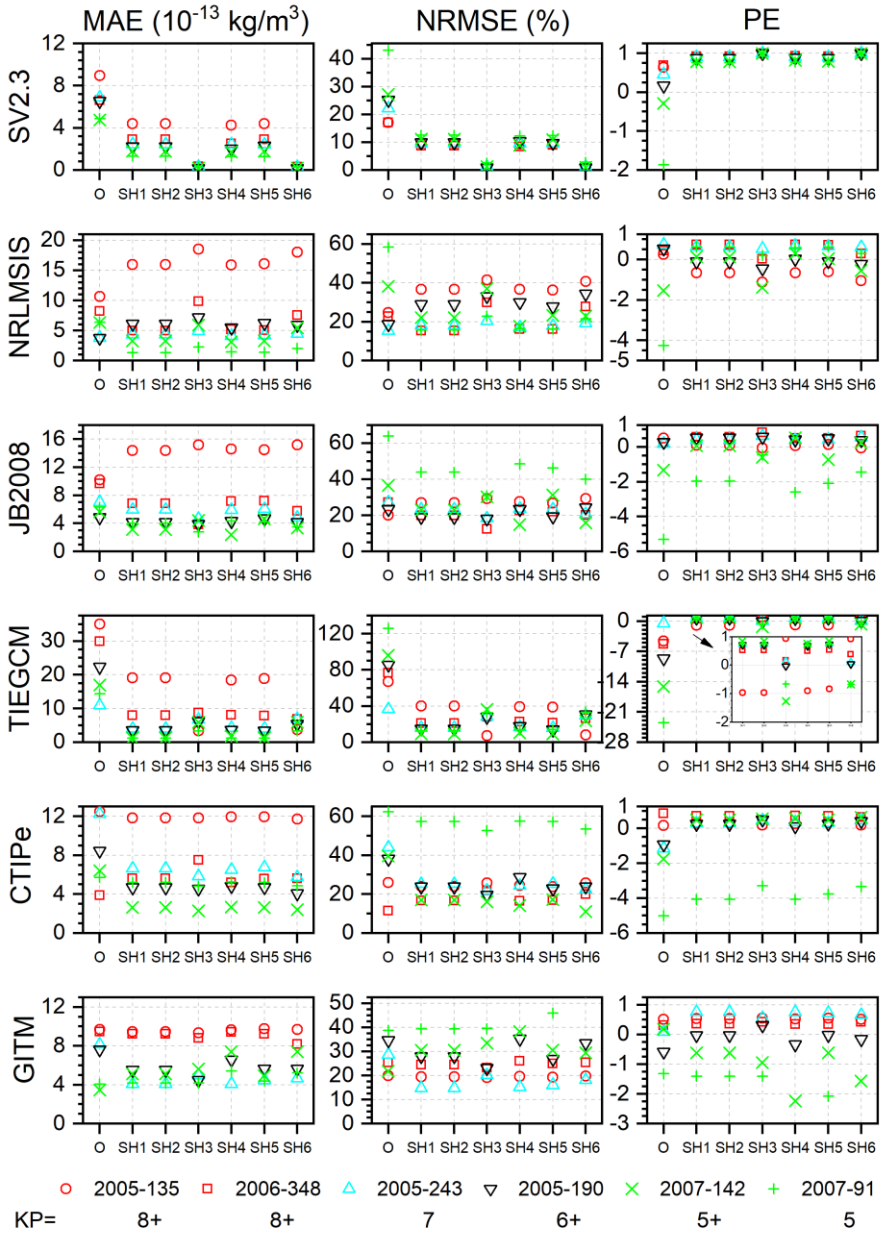

Figure S11: The expanded form of Figure5 with all shifts. O denotes the results for the original, unshifted series whereas SH1 to SH6 represent the shifts from Shift1 to Shift6. The color coding and symbols are the same as Figure S8.

Event	Simulation IDs in CCMC Runs on Request System	Model Name and Version	Resolution (lat × long)
2006-348	Emine_Kalafatoglu_110113_IT_1	TIEGCM 1.95	2.5° × 5°
	Emine_Kalafatoglu_112613_IT_1	GITM 2.0	2.5° × 5°
	JaSoon_Shim_061114_IT_1	CTIPe	2° × 18°
2005-135	Emine_Kalafatoglu_050714_IT_2	TIEGCM 1.95	2.5° × 5°
	Emine_Kalafatoglu_051314_IT_1	GITM 2.0	2.5° × 5°
	Emine_Kalafatoglu_070314_IT_3	CTIPe	2° × 18°
2005-243	Emine_Kalafatoglu_050814_IT_1	TIEGCM 1.95	2.5° × 5°
	Emine_Kalafatoglu_051414_IT_1	GITM 2.0	2.5° × 5°
	JaSoon_Shim_061114_IT_2	CTIPe	2° × 18°
2005-190	Emine_Kalafatoglu_050714_IT_4	TIEGCM 1.95	2.5° × 5°
	Emine_Kalafatoglu_051314_IT_2	GITM 2.0	2.5° × 5°
	JaSoon_Shim_061114_IT_3	CTIPe	2° × 18°
2007-142	Emine_Kalafatoglu_050914_IT_3	TIEGCM 1.95	2.5° × 5°
	Emine_Kalafatoglu_051314_IT_3	GITM 2.0	2.5° × 5°
	Emine_Kalafatoglu_070714_IT_1	CTIPe	2° × 18°
2007-091	Emine_Kalafatoglu_050914_IT_2	TIEGCM 1.95	2.5° × 5°
	Emine_Kalafatoglu_051514_IT_2	GITM 2.0	2.5° × 5°
	Emine_Kalafatoglu_070714_IT_2	CTIPe	2° × 18°

Table S1. Model runs at the CCMC for each event

Model Name	Model Type	Model Inputs
NRLMSIS	Empirical	F10.7, daily Ap, 3 hourly ap
JB2008	Empirical	Dst, ap, F10.7, S10.7, M10.7, Y10.7
TIEGCM	Physics-based	F10.7, 81-day center averaged F10.7 (F107A), Hemispheric Power for usage with Weimer: IMF B_x, B_y, B_z, solar wind speed, for tides: GSWM
CTIPe	Physics-based	F10.7, ACE Level 2 solar wind data, Earth's dipole tilt angle, NOAA/POES hemispheric power data
GITM	Physics-based	F10.7, Solar irradiance, Hemispheric Power index, Weimer electric field, Fuller Rowell and Evans (1987) for auroral precipitation pattern, MSIS and IRI for the initial state of the thermosphere. For usage with Weimer: IMF B_x, B_y, B_z, solar wind speed, for tides: GSWM

Table S2. Input to models

Event	Model	ρ_{avg}	$\Delta\rho$
2005-135	SV2.3	2,92E-12	4,55E-13
	MSIS	3,53E-12	1,06E-12
	JB2008	2,95E-12	4,83E-13
	TIEGCM	4,11E-12	1,64E-12
	CTIPe	3,01E-12	5,44E-13
	GITM	2,54E-12	7,02E-14
	M2017	2,47E-12	0
2006-348	SV2.3	2,40E-12	3,72E-13
	MSIS	3,32E-12	1,30E-12
	JB2008	2,46E-12	4,31E-13
	TIEGCM	4,61E-12	2,58E-12
	CTIPe	2,41E-12	3,86E-13
	GITM	2,11E-12	8,02E-14
	M2017	2,03E-12	0
2005-243	SV2.3	2,56E-12	4,45E-13
	MSIS	2,30E-12	1,81E-13
	JB2008	2,30E-12	1,77E-13
	TIEGCM	3,45E-12	1,33E-12
	CTIPe	2,95E-12	8,29E-13
	GITM	2,89E-12	7,71E-13
	M2017	2,12E-12	0
2005-190	SV2.3	2,67E-12	4,30E-13
	MSIS	2,68E-12	4,36E-13
	JB2008	2,63E-12	3,93E-13
	TIEGCM	4,47E-12	2,23E-12
	CTIPe	2,78E-12	5,42E-13
	GITM	2,47E-12	2,26E-13
	M2017	2,24E-12	0
2007-142	SV2.3	1,78E-12	2,95E-13
	MSIS	2,44E-12	9,58E-13
	JB2008	2,19E-12	7,03E-13
	TIEGCM	3,28E-12	1,80E-12
	CTIPe	2,01E-12	5,27E-13
	GITM	1,65E-12	1,66E-13
	M2017	1,48E-12	0
2007-91	SV2.3	2,04E-12	3,57E-13
	MSIS	2,30E-12	6,12E-13
	JB2008	1,98E-12	2,89E-13
	TIEGCM	3,09E-12	1,40E-12
	CTIPe	1,76E-12	7,66E-14
	GITM	1,69E-12	8,03E-15
	M2017	1,69E-12	0

Table S3. Quiet-time averages of the model and observations and the mean difference between the M2017 and models that were used for SH1 and SH2.